Journal of
Composites Science

MDPI

Article

Effect of Mechanical Recycling on the Mechanical Properties of PLA-Based Natural Fiber-Reinforced Composites

James Finnerty [1,*], Steven Rowe [1], Trevor Howard [1], Shane Connolly [1], Christopher Doran [1], Declan M. Devine [2], Noel M. Gately [1], Vlasta Chyzna [3], Alex Portela [3], Gilberto Silva Nunes Bezerra [2], Paul McDonald [4] and Declan Mary Colbert [2,*]

[1] Applied Polymer Technology Gateway, Technological University of the Shannon, University Road, N37HD68 Athlone, Ireland
[2] PRISM Research Institute, Technological University of the Shannon, University Road, N37HD68 Athlone, Ireland
[3] Centre for Industrial Services and Design, Technological University of the Shannon, University Road, N37HD68 Athlone, Ireland
[4] Department of Polymer, Mechanical & Design, Technological University of the Shannon, University Road, N37HD68 Athlone, Ireland
* Correspondence: james.finnerty@tus.ie (J.F.); declan.colbert@tus.ie (D.M.C.)

Abstract: The present study investigates the feasibility of utilizing polylactic acid (PLA) and PLA-based natural fiber-reinforced composites (NFRCs) in mechanical recycling. A conical twin screw extrusion (CTSE) process was utilized to recycle PLA and PLA-based NFRCs consisting of 90 wt.% PLA and a 10 wt.% proportion of either basalt fibers (BFs) or halloysite nanotubes (HNTs) for up to six recycling steps. The recycled material was then injection molded to produce standard test specimens for impact strength and tensile property analysis. The mechanical recycling of virgin PLA led to significant discoloration of the polymer, indicating degradation during the thermal processing of the polymer due to the formation of chromatophores in the structure. Differential scanning calorimetry (DSC) analysis revealed an increase in glass transition temperature (T_g) with respect to increased recycling steps, indicating an increased content of crystallinity in the PLA. Impact strength testing showed no significant detrimental effects on the NFRCs' impact strength up to six recycling steps. Tensile testing of PLA/HNT NFRCs likewise did not show major decreases in values when tested. However, PLA/BF NFRCs exhibited a significant decrease in tensile properties after three recycling steps, likely due to a reduction in fiber length beyond the critical fiber length. Scanning electron microscopy (SEM) of the fracture surface of impact specimens revealed a decrease in fiber length with respect to increased recycling steps, as well as poor interfacial adhesion between BF and PLA. This study presents a promising initial view into the mechanical recyclability of PLA-based composites.

Keywords: recycling; brabender; extrusion; injection molding; sustainable

Citation: Finnerty, J.; Rowe, S.; Howard, T.; Connolly, S.; Doran, C.; Devine, D.M.; Gately, N.M.; Chyzna, V.; Portela, A.; Bezerra, G.S.N.; et al. Effect of Mechanical Recycling on the Mechanical Properties of PLA-Based Natural Fiber-Reinforced Composites. *J. Compos. Sci.* **2023**, *7*, 141. https://doi.org/10.3390/jcs7040141

Academic Editor: Francesco Tornabene

Received: 1 March 2023
Revised: 16 March 2023
Accepted: 31 March 2023
Published: 6 April 2023

1. Introduction

Though consumers may think of recycling as a singular action, in reality recycling can be subdivided into four categories: primary (1°), secondary (2°), tertiary (3°) and quaternary (4°); 1° recycling refers to the utilization of pure or pre-consumer polymer materials; 2° recycling, meanwhile, involves the sorting of waste streams, washing, shredding and re-extrusion of polymer waste; 3° recycling, also known as chemical recycling, refers to the chemical breakdown of polymer waste into its monomers which may be subsequently re-polymerized, thereby reproducing virgin polymer; 4° recycling is by far the least environmentally friendly option as it refers to the transformation of plastic waste into energy through processes such as pyrolysis. There is an ever-growing emphasis on the recyclability of polymeric materials as global consumption of plastics continues to rise,

projected to reach 460 million tons per annum by the year 2030 [1]. This will not only inevitably lead to the generation of vast volumes of plastic waste but also lead to significant increases in greenhouse gas (GHG) emissions. This was highlighted by both Zhang et al. (2020) and Shen et al. (2020) who discussed the growth in GHG emissions attributed to plastics potentially reaching 1.34 gigatons (Gt) per annum by 2030 [2,3]. In response to these growing environmental issues relating to plastic use, the implementation of national regulations regarding the use and disposal of plastics has become a global trend [4,5].

As a response to these trends, there has been an ever-growing interest in the use of sustainable biopolymers. Biopolymers are polymeric materials wherein at least one monomer is derived from renewable sources or may be biodegradable regardless of its origin [6]. Though there are numerous biopolymers available, one of the most commonly used biopolymers in the plastics packaging market is polylactic acid (PLA), chemically synthesized from monomers derived from natural resources such as maize, wheat and cassava [7,8]. Though PLA may be produced from lactic acid, it is most commonly synthesized via ring opening polymerization (ROP) of its cyclic dimer, lactide [9]. The popularity of PLA as a biopolymer is not only due to its wide availability and relatively low price but also due to PLA being comparable to common engineering plastics such as polypropylene (PP) and polyethylene terephthalate (PET) in terms of mechanical and physical properties [10]. PLA has a glass transition temperature (T_g) range of 50–70 °C [11] and a melting temperature (T_m) of between 145 and 170 °C [12,13]. Maintaining a Tg in this high range may lead to a brittle final product when produced using a melt-processing production method [14].

One of the most common methodologies in enhancing the mechanical properties of polymer-based products is to create polymer/fiber composites. Similar to the issues with polymers though, the use of synthetic fibers as the composite material will also present environmental concerns. This issue may be overcome through the use of natural fibers (NFs). NFs are an incredibly broad category of materials though they may be summarized as fibers which are not synthetically created. Pilla et al. (2009) manufactured molded natural composites of PLA and recycled wood fibers (RWF) [15]. It was shown that though the addition of RWF increased the tensile modulus of samples, the RWF lead to a significant decrease in the toughness of samples compared to that of neat PLA. Bajpal et al. (2012) showed that the incorporation of a 20 wt.% loading of sisal fibers improved the tensile, impact and flexural properties by 80.6 MPa, 106 kJ/m^2 and 249.8 MPa, respectively [16]. The incorporation of various volume fractions of kenaf, hemp and jute fibers has been shown to also increase the mechanical properties of PLA-based composites [17–19]; a 30 vol.% of jute fibers was shown to be the optimal volume fraction for improvements in tensile and flexural properties [19]. Two natural fiber materials of great interest for fiber reinforcement of polymers are basalt fibers (BFs) and halloysite nanotubes (HNTs).

The interest in BFs as reinforcement fibers has predominantly been due to the fibers being non-toxic, easy to process, renewable, being relatively cheaper in comparison to other reinforcing fibers as well as possessing excellent technical properties [20,21]. BFs predominantly comprise oxides such as silicon dioxide (SiO_2), aluminum oxide (Al_2O_3), calcium oxide (CaO), and magnesium oxide at proportions of 45 ± 1 wt.%, 12 ± 1 wt.%, 11 ± 1 wt.% and 10 ± 1 wt.%, respectively [22].

HNTs are naturally occurring aluminosilicate clay which present as tubular-shaped particles and are abundantly available in nature [23,24]. HNTs have a dimensional morphology consisting of a single tetrahedral sheet and an octahedral sheet [25,26]. The tetrahedral layer of the HNTs is negatively charged and is composed of siloxane groups (Si-O-Si and Si-OH) at the outermost surface. The octahedral sheets, meanwhile, comprise positively charged gibbsite aluminol groups (Al-OH) at the innermost surface [27].

Considering the growing research interest in the areas of HNT- and BF-reinforced composites (HNTRC and BFRC), the presented work concerns an initial assessment of the effect of mechanical recycling on the mechanical performance of PLA and PLA-based NF-composites. The objectives of this study were to examine whether BF- and HNT-based NFRCs could be mechanically recycled via an extrusion process while maintaining a high degree of mechanical strength imposed on composites by the contained fibers. In the current study, BFs and HNTs were incorporated into the polymer matrix and mechanically recycled up to six times in total and the mechanical properties were evaluated. It is hoped that this work will lead to increased focus on the recyclability of PLA-based materials as opposed to solely composting the material, thus improving the waste management options available.

2. Materials and Methods

2.1. Materials

Polylactic acid (PLA) was supplied from NatureWorks in pellet form. It had a density of 1.24 g/cm^3, a T_m of 155–170 °C and a tensile modulus of 3447 MPa. Sigma-Aldrich supplied the halloysite nanotubes (HNTs) in powder form. They had a density of 2.56 g/cm^3, a cylindrical form with a length of 0.2–2 µm, an outer diameter of 50–70 nm, an inner diameter of 15–45 nm, and a length-to-diameter ratio of 10:20. The basalt fibers (BFs) were BASFIBER® supplied by Basalt Fiber Tech. They had a linear density range of 270–4800 tex, a moisture content < 0.1 wt.% and a T_m range of 1460–1500 °C.

2.2. Preparation of PLA/PLA-Based Composites

All materials were pre-dried for 4 h at 80 °C prior to hot melt-extrusion (HME) and injection molding (IM). The materials were weighed using an Ohaus 7000 Series balance and subsequently placed into sealed polyethylene bags. The sealed bags were then manually tumble mixed for 5 min to ensure a homogenous mixture. The blend compositions are shown in Table 1.

Table 1. Blend compositions prepared for this study.

Sample Name	PLA (wt.%)	HNT (wt.%)	BF (wt.%)
PLA90/HNT10	90	10	-
PLA90/BF10	90	-	10

2.3. Hot Melt Extrusion of Composites

All melt processing for the production of natural fiber-reinforced composites (NFRCs) in this research study was carried out on a Brabender MetaStation 4E (Duisburg, Germany) with a conical twin screw extruder (CTSE) attachment possessing a screw diameter of 32/30 mm and a screw length of 342 mm (Figure 1). The extrudate was formed into a strand via an attached 5 mm filament die. The Brabender used for this research study is owned by and located in the Applied Polymer Technology Gateway (APT) situated in the Athlone campus of the Technological University of the Shannon Midlands Midwest. The barrel temperature profile used was kept constant between formulations at 150/160/170/180/190/200 °C from Zone 1 to Die with a constant screw rotational speed of 50 RPM. These parameters allowed for a material throughput of ~1.5 kg h^{-1}. Post-extrusion, the extrudate was cooled on a pressurized air-cooling conveyor system and granulated using a bench-top Prism granulator to obtain pellets ~5 mm in length. The three material blends trialed (Table 1) were extruded a total of six times to observe the effect of mechanical recycling on the characteristics of the extrudate.

Figure 1. (**Left**) Brabender conical twin screw extruder and (**Right**) Co-rotating conical screws.

2.4. Injection Molding

Injection molding of impact and tensile bars was performed on an Arburg Allrounder 370 E located in Applied Polymer Technologies. After each recycling step, a proportion of material was retained to undergo injection molding to produce samples denoted as being recycled 1, 3 or 6 times. The Arburg has a maximum clamping force of 600 kN with a screw diameter of 30 mm and a theoretical stroke volume of up to 85 cm^3. The temperature profile was established by means of four temperature controllers placed along the length of the barrel with a fifth temperature controller used to regulate the temperature at the nozzle. The temperature profile used was similar to that of the extrusion process proceeding from 160 °C at the hopper to 200 °C at the nozzle and a cooling time of 30 s. The mold was maintained at 30 °C by means of a separate mold temperature control unit. The mold utilized for the production of test specimens was a "two by two" mold, for the production of both tensile and impact test specimens, with a shot size of 28 g. The molded NFRCs are shown in Figure 2.

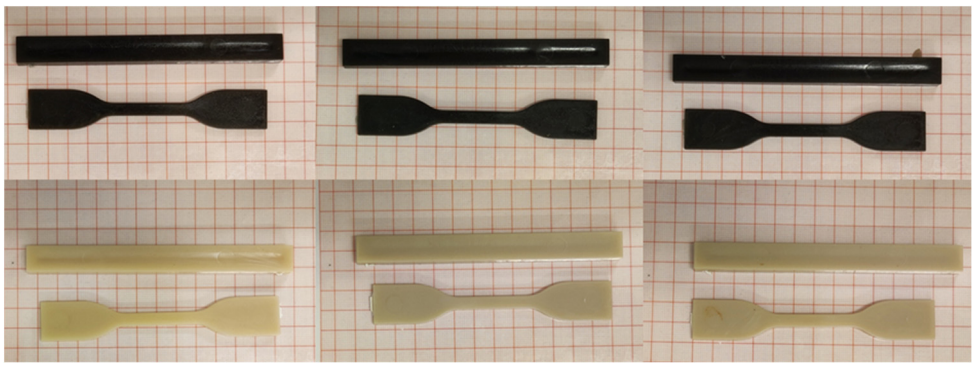

Figure 2. Injection-molded tensile and impact test specimens. (**Top row Left–Right**) PLA90%BF10% after 1, 3 and 6 recycling steps; (**Bottom row Left–Right**) PLA90%HNT10% after 1, 3 and 6 recycling.

2.5. Thermal Analysis via Differential Scanning Calorimetry

DSC analysis was carried out using a Pyris 6 DSC (PerkinElmer, Waltham, MA, USA), which was calibrated using indium as the reference material. Samples between 6 and 8 mg were accurately measured and placed in lid-sealed aluminum pans. Calorime-try scans were performed using a heating rate of 10 °C min^{-1} applying standard heat from 20 to 300 °C min^{-1} for the PLA that had undergone 1, 3 and 6 recycling steps. Samples were tested under nitrogen atmosphere with a flow of 30 mL min^{-1} to avoid oxidation. The percentage of crystallinity (χ_c) of the various PLA samples was determined using Equation (1).

$$\chi_c = \frac{\Delta H}{\Delta H^*} \quad (1)$$

2.6. Morphology of Fracture Surface

The morphology of the fracture surface of injection-molded impact bars was evaluated using a scanning electron microscope (Tescan Mira, Oxford Instruments, Cambridge, UK). Prior to imaging, samples were attached to an adhesive conducting tape on the stubs and subsequently sputtered with gold utilizing a Baltec SCD 005 sputter coater (BAL-TEC GmbH, Schalksmühle, Germany).

2.7. Color Measurement

The influence of mechanical recycling on the color of virgin PLA was carried out in a Lovibond reflectance tintometer (Dortmund, Germany). The color coordinates L^*, a^* and b^* were collected. L^* is representative of luminance (from black to white), a^* represents the transition from green to red and b^* the transition from blue to yellow. Prior to testing the PLA samples, the colorimeter was calibrated with a white standard tile and a mirror to represent black. The white color standard with coordinate values $L^*a^*b^*$ were obtained on five different samples and the corresponding average values and standard deviations were calculated. From this coordinate, it was possible to determine the color difference associated with this space. The distance metric, ΔE^*_{ab}, was obtained by following Equation (2) and compared with the color coordinates of the initially recycled PLA sample used as reference. The yellowness index (YI) was automatically generated from the determined coordinates by OnColor software.

$$\Delta E^*_{ab} = \sqrt{(\Delta L^*)^2 + (\Delta a^*)^2 + (\Delta b^*)^2} \quad (2)$$

2.8. Charpy Impact Testing

A calibrated Zwick Roell CEAST 6545 (Zwick Roell, Ulm, Germany) was used to carry out a Charpy notched impact test on a total of 6 samples. Test specimens, with an average thickness of 12.72 mm (±0.04 mm), were notched to a depth of 0.5 mm and then placed in the sample holder. A 4 Joule hammer attachment was used and initially zeroed by releasing the arm with no samples in the holder. The sample was then placed with the notch placed as centrally to the arm as possible. The hammer arm was then locked in the upward position and subsequently released. The resultant downswing of the arm provides the impact energy of the test specimen in J. The impact strength of samples was subsequently calculated using Equations (3) and (4), where K = notch impact energy, m = mass of hammer, g = gravity constant, A = cross-sectional area and $\propto$ = notch toughness.

$$K = m \times g \times (H - h) \quad (3)$$

$$\propto = \frac{K}{A} \quad (4)$$

2.9. Tensile Testing

Tensile testing was performed in accordance with EN ISO 527 standard for test specimens using an Instron tensile tester (Instron, Norwood, MA, United States). A total of 6 specimens for each sample were tested, with dimensions of 170 mm in length, a width of 10 ± 0.2 mm, and a thickness of 4 ± 0.2 mm. The tensile testing was performed under quasi-static conditions at ambient room temperature, approximately 20 °C. The tensile properties were obtained directly from the machine.

3. Results

3.1. Physical Appearance of Recycled PLA

The physical appearance of granulated virgin PLA after 1, 3 and 6 mechanical recycling steps is presented in Figure 3. It is evident that as the number of extrusion steps increased so too did the darkening of the yellow color. This yellowing of the virgin material

during reprocessing can be an important factor in the end-usage of PLA from a consumer perspective especially in packaging applications. This yellowing of PLA after numerous reprocessing steps has been described extensively in the literature [28–31]. In general, there is an association between color formation and degradation. Hopmann et al. (2014) noted the increase in "yellowing" with increased thermal processing steps there being due to unavoidable thermal degradation of the PLA which leads to a chemical reaction occurring. These chemical reactions—the formation of chromophores whose conjugated double bonds are capable of absorption on higher wavelengths—are thus responsible for the yellowing of the PLA [28,31]. The appearance of injection-molded specimens of PLA subjected to the various recycling steps is shown in Figure 4. As with the granulated material, as the number of recycling steps increased, so too did the tendency of samples to display a pronounced yellow coloration [32,33].

Figure 3. Granulated virgin PLA after recycling process; (**Left–Right**) 1 recycling, 3 recycling and 6 recycling steps.

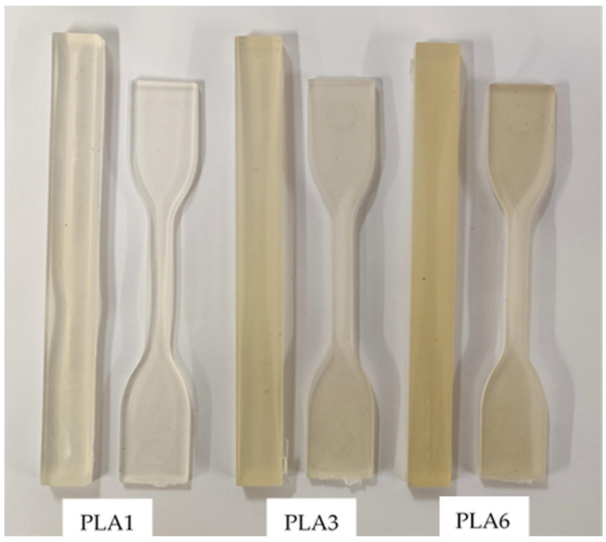

Figure 4. Injection-molded samples of PLA post 1, 3 and 6 recycling steps. The samples are noticeably more yellow with respect to increased recycling steps.

Simple visual evaluation with the naked eye of Figures 3 and 4 reveals the clear evidence of the effect of additional recycling steps on the change in color of the PLA material. Table 2 displays the color coordinates (L^*a^*b), the variance in color determined by ΔE^*_{ab} with respect to the PLA sample post 1-recycling step. The yellowness index (YI) was assessed by ASTM standard (D65/10°) where YI indicates the transition in color from white to yellow.

Table 2. Color parameters of injection-molded samples of PLA after being subjected to varying degrees of mechanical recycling.

No. of Recycling Steps	L^*	a^*	b^*	ΔE^*_{ab}	YI
1	77.01 (±2.38)	0.29 (±0.03)	4.63 (±1.80)	-	10.69 (±1.50)
3	73.31 (±1.80)	0.22 (±0.02)	8.41 (±0.33)	5.41 (±1.32)	19.60 (±0.75)
6	70.08 (±1.07)	0.32 (±0.01)	11.50 (±0.28)	9.35 (±1.00)	26.44 (±0.51)

As would be expected, the value for L^* decreases with respect to additional recycling steps, thus indicating a decrease in the brightness of samples. Additionally, there is a noted sharp increase of 248.38% in the value of b^* (shift from blue to yellow) as recycling goes from one step to six steps. The values of ΔE^*_{ab} denote whether the change in color is noticeable to the eye and to what extent; where a ΔE^*_{ab} <1 denotes an unnoticeable color change, ≥1 and <2 denotes a change noticeable only to an experienced observer, ≥2 and <3.5 denotes a change noticeable to an unexperienced observer, ≥3.5 and <5 display a clear noticeable difference and ≥5 displays noticeably different colors to an observer [34,35]. The tested samples displayed values >5 for ΔE^*_{ab} with respect to the initial sample (PLA recycled a single time); 5.41 and 9.35 for PLA recycled three times and six times, respectively. The YI of tested samples progresses upwards from 10.69 (PLA one recycling step) to 26.44 (PLA six recycling steps). Such values indicate that the samples are noticeably a different color to the original test specimen with an increasing tendency to yellow with respect to additional processing cycles, as is clearly evident when observing Figures 3 and 4. These results are in corroboration with those found in the literature [29,36].

3.2. Thermal Characterisation of Recycled PLA

DSC analyses (Figure 5 and Table 3) were carried out to investigate the thermal properties of the recycled PLA material. Aliphatic polyesters, such as PLA, are known to be especially sensitive to hydrolytic degradation processes owing to the effect of moisture on the ester groups. This effect is amplified when under the effect of increased temperature. The recycling of PLA thereby increases its sensitivity to moisture [37]. As such, DSC analysis is a useful tool in identifying the various thermal transitions of PLA subjected to different recycling processes.

It can be seen that the increase in the number of recycling steps from 1 to 6 affected the glass transition temperature (T_g) of PLA from 61.44 to 69.39 °C, an increase of approximately 8 °C. The literature attributes this phenomenon to a reduction in the free volume and restriction on the motion of the polymeric chains [38,39]. Moreover, neat PCL is known for not exhibiting a crystallization peak upon cooling as a consequence of a slow crystallization rate. In this study, none of the recycled PLA materials exhibited either, which is not a desirable behavior to the production of pieces with higher dimensional stability [38]. The crystallization temperature on heating (T_{cc}) was present for the recycled material under one recycling step; nevertheless, this exothermic peak of crystallization disappeared as we increased the number of recycling steps.

Furthermore, an increase was observed in the crystallinity degree of 42.49% from one recycling step to 57.81% from three recycling steps, which indicates crystallization of the polymeric material after the recycling process [38], whilst the slight reduction to 55.55% can be related to the polymer molecular weight variation due to the thermal and mechanical stresses, leading to melt fracture [40]. This information can be endorsed by the increase in the melting temperature (T_m) of the recycled PLA material from 170.48 °C (ΔH_m = 39.52 J g^{-1}) to 172.13 °C (ΔH_m = 53.77 J g^{-1}), followed by a slight reduction to 171.49 °C (ΔH_m = 51.72 J g^{-1}), respectively. It has been reported that the melting temperature is highly dependent on the crystallinity of the polymeric material [38]. Thus, based on the increase in the melting temperature and crystallinity of the recycled PLA material, it can be assumed that the recycling process from one to three steps enhanced the

crystallization rate and improved the quality of the crystals; however, after six recycling steps these properties added to the material decline.

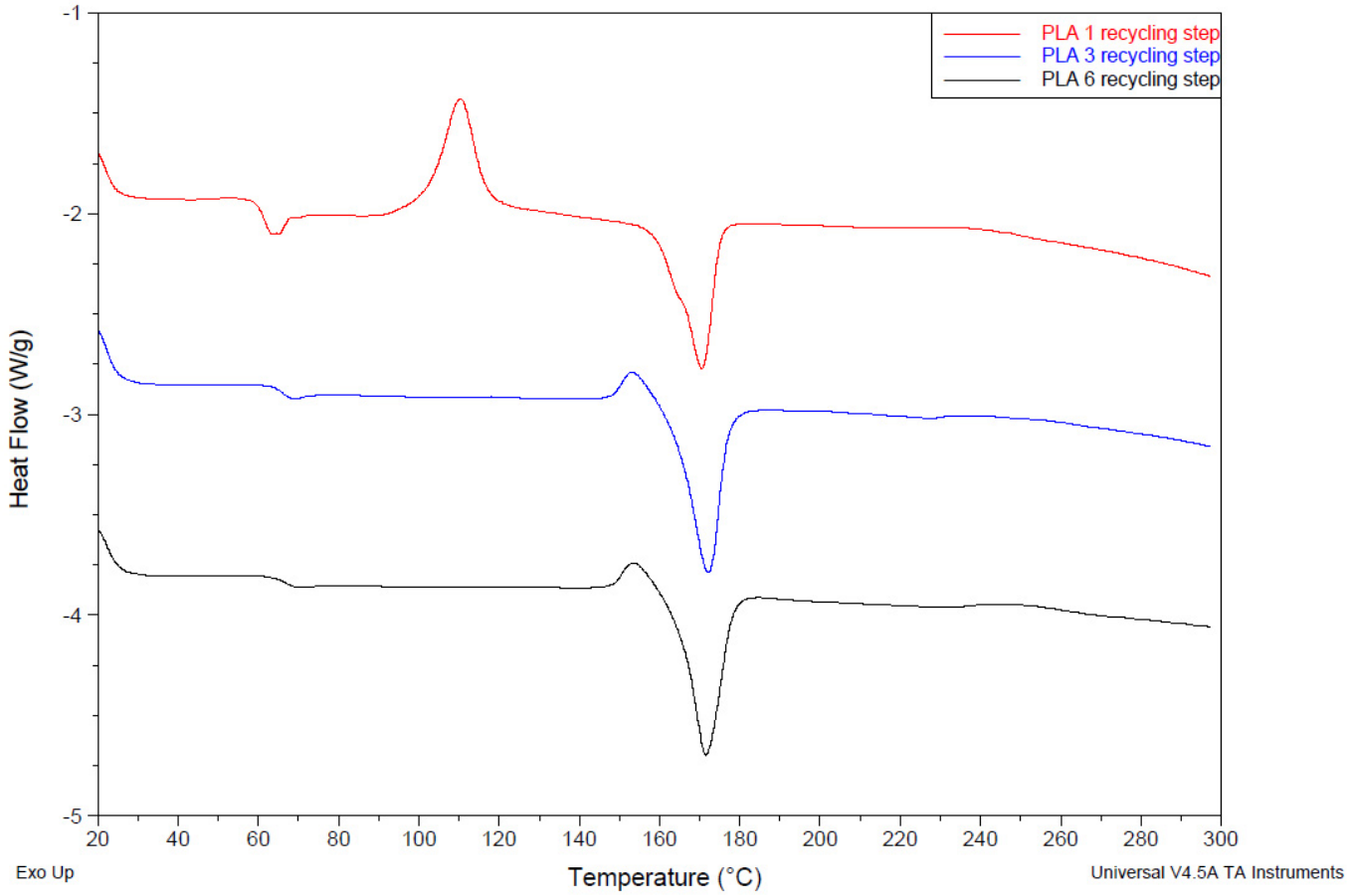

Figure 5. Overlay thermogram of the PLA material after undergoing 1, 3 and 6 mechanical recycling steps.

Table 3. Thermal properties observed via DSC of the recycled PLA material.

No. of Recycling Steps	T_g (°C)	ΔH_{cc} (J g^{-1})	T_{cc} (°C)	ΔH_m (J g^{-1})	T_m (°C)	X_c (%)
1	61.44	36.65	110.16	39.52	170.48	42.45
3	66.03	-	-	53.77	172.13	57.76
6	69.39	-	-	51.72	171.49	55.55

$X_c = (\Delta H/\Delta H^*)$; ΔH is the melting enthalpy calculated through integration of the melting peak determined via DSC; $\Delta H^* = 93.1$ J g^{-1} is the melting enthalpy of a 100% crystalline PLA [41].

3.3. Tensile Properties of PLA and PLA-Based Composites

The tensile properties of an NFRC are highly dependent on a variety of factors including the compatibility between the fiber and chosen polymer matrix, the molecular weight of the polymer and the fiber aspect ratio. Reprocessing of NFRCs, however, will not have a singular effect as studies have shown that the tensile properties of reprocessed samples may improve or worsen with respect to reprocessing cycles. The tensile strength of recycled LDPE/waste cotton textile composites has been shown to initially increase and subsequently decrease with additional reprocessing steps [42]. The authors noted that the initial increase in tensile strength of the NFRCs may be attributed to the fiber aspect ratio increasing during reprocessing, thus leading to higher dispersion in the polymer matrix. Such a trend was observed herein for the NFRCs of PLA90/HNT10. Going from one recycling step to three recycling steps, there is an initial increase in tensile stress at

a break of 4.4% while subsequent recycling steps lead to a reduction in tensile stress at a break of 1.1%. This trend is similar across both tensile strain at break and Youngs Modulus for the aforementioned samples as displayed in Table 4 and Figure 6. The tensile properties of the HNT-loaded composites are quite interesting. As can be seen in Table 5, the tensile stress at break for PLA90/HNT10 increases by 4.41% when comparing recycling step 3 to recycling step 1 and increases by 3.27% when comparing recycling step 6 to recycling step 1. This increase in tensile stress could be ascribed to the increase in polymer crystallinity during the reprocessing cycles. As crystallinity is known to increase as a result of chain scission and, therefore, a reduction in molecular weight, it could be inferred that the multiple re-processing steps have led to a reduction in PLA molecular chain length [43]. This would seem to agree with the results of this study as crystallinity is known to have a direct influence on tensile strength and the elastic properties of materials. As crystallinity increases, so too does sample strength as within the crystalline phase of polymers the intermolecular bonding is more significant than in the amorphous phase [44]. The effect of recycling steps on the crystallinity of injection-molded samples has similarly been shown by Huang and Peng (2021). In this study on the effect of recycling times on the tensile properties of injection-molded polypropylene (PP), the crystallinity of samples was shown to increase from ~38% to ~47% after five recycling steps [43].

Table 4. Tensile properties of tested samples (n = 6). (σ) tensile stress at break, (ε) tensile strain at break and (E) Young's Modulus.

Sample	No. of Recycling Steps	σ (MPa)	ε (%)	E (MPa)
PLA90 /HNT10	1	67.41 (±1.14)	3.28 (±0.11)	2728.60 (±94.85)
	3	70.38 (±2.43)	4.53 (±0.12)	2792.62 (±77.35)
	6	69.61 (±0.92)	3.38 (±0.08)	2684.73 (±45.58)
PLA90 /BF10	1	83.79 (±1.05)	3.72 (±0.11)	3176.44 (±35.12)
	3	66.93 (±1.83)	3.34 (±0.06)	2876.88 (±116.08)
	6	69.61 (±1.40)	3.46 (±0.10)	2820.88 (±60.04)

Table 5. Impact strength results of tested samples (n = 6).

Sample	No. of Recycling Steps	Impact Strength (kJ/m^2)
PLA90/HNT10	1	3.950 (±0.23)
	3	3.773 (±0.47)
	6	3.255 (±0.49)
PLA90/BF10	1	4.837 (±0.48)
	3	4.249 (±0.45)
	6	4.168 (±0.13)

The testing revealed the HNT to have a reinforcing effect on the PLA wherein the incorporation of HNT resulted in a large increase in Youngs Modulus regardless of recycling step; PLA90/HNT10 after one recycling step 2728.6 MPa, PLA90/HNT10 three recycling steps 2792.62 MPa and PLA90/HNT10 six recycling steps 2684.73 MPa. Interestingly, the HNT-loaded composites displayed a lower tensile stress than the virgin polymer. This is similar to the results obtained by Chen et al. (2015). This team of researchers reported a 5% loading of HNT to yield the greatest increase in strength of PLA composites, with further loading yielding a reduction in tensile stress from this maximum. The reinforcing effect of the HNT is believed to be due to the fact that the fiber length of the HNT is smaller than the critical crack length which may typically initiate failure within a polymer composite and, therefore, improves the strength of the sample [45]. As can be seen, these values begin to decline at recycling step 6. This is likely due to the increased amount of

processing steps leading to a reduction in fiber length, as it is well known that tensile strength generally increases with increasing fiber length up to a critical point at which it has minimal effect on the tensile strength [46].

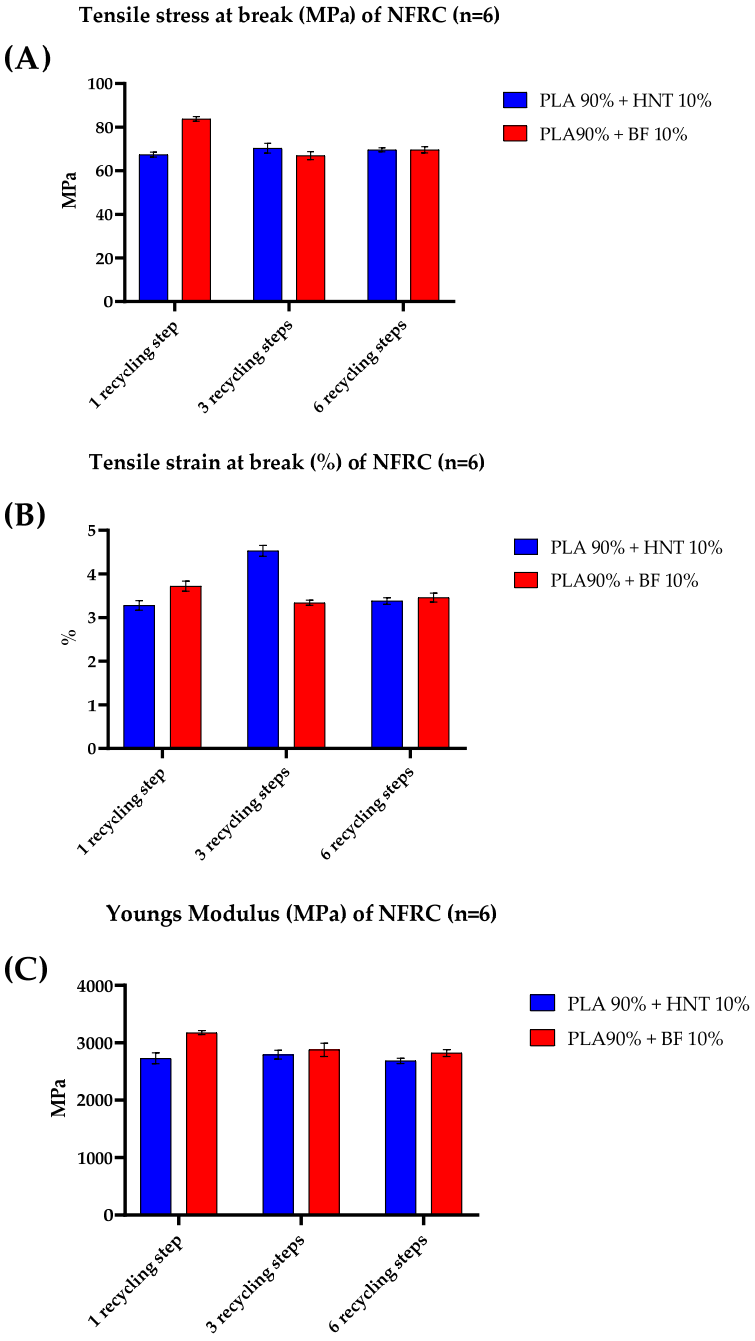

Figure 6. Values of tensile properties of all tested samples (n = 6). (**A**) tensile stress at break of samples. (**B**) tensile strain at break of samples and (**C**) Youngs Modulus of samples; (blue) PLA 90 wt.% and HNT 10 wt.% and (red) PLA 90 wt.% and BF 10 wt.%. Error bars represent standard error of the mean.

PLA90/BF10 displayed an inverse trend whereby initially there was a large reduction in tensile properties going from one to three reprocessing steps followed by a subsequent slight increase going from three to six reprocessing steps. Going from one recycling step to three recycling steps led to a decrease in tensile stress of 20.12%, a decrease in tensile strain of 10.13% and reduction in Youngs Modulus of 9.43%. Meanwhile, comparing recycling

step 1 to recycling step 6 there is a reduction of 16.91%, 6.95% an 11.19% for tensile stress, tensile strain and Youngs Modulus, respectively.

The effect of reprocessing steps on the tensile properties cannot simply be explained as being due to a singular effect, but may be the summation of several coinciding processes. At temperatures exceeding 50°C, PLA is known to be particularly susceptible to hydrolytic degradation due to present moisture. NFs are known to retain high degrees of moisture content regardless of drying. This effect was shown by Graupner et al. (2016) whereby they compared PLA-based NFRCs with recycled PLA-based NFRCs with identical fiber length distributions. The mechanical properties of the non-recycled composites far exceeded that of the recycled composites, thereby showing that the breakage of fibers was not the sole contributing factor [47]. Additional studies utilizing cellulose filler or wood fiber displayed that the degradation of PLA was accelerated with respect to increasing loading of fiber/filler as the higher quantity of reinforcement material contained higher quantities of moisture [48,49].

The choice of fibers is an important choice to make as certain natural fibers used in PLA-based NFRCs can cause a reduction in tensile properties. Coffee grounds (CG) and bamboo flour (BBF), for instance, when incorporated into a PLA matrix lead to a reduction in tensile strength compared to the virgin polymer due to weak interface and obstruction of stress concentration [50]. Kumar and Tumu (2019) showed similar trends wherein the reduction in tensile strength is noted as being due to poor interfacial compatibility between the polymer matrix and BBF as well as poor dispersion of the bamboo fibers [51].

The tensile properties of reprocessed PLA-based composites are shown in Table 5 and presented graphically in Figure 4. When observing the samples of virgin PLA, there is a decrease of 2.54% in the tensile stress of samples going from one recycling step to three recycling steps, yet an increase of 4.08% in the tensile stress going from one recycling step to six recycling steps. The tensile strain meanwhile yields reductions of 6.02% and 2.68% given the same timepoints.

The tensile properties of the BF-loaded composites were greatly affected by mechanical recycling. Going from one recycling step to three recycling steps led to a decrease in tensile stress of 20.12%, a decrease in tensile strain of 10.13% and reduction in Youngs Modulus of 9.43%. Meanwhile, comparing recycling step 1 to recycling step 6 there is a reduction of 16.91%, 6.95% and 11.19% for tensile stress, tensile strain and Youngs Modulus, respectively. The large decrease in tensile properties of the BF composites can once again likely be explained by a reduction in fiber length during the reprocessing steps. Going from recycling step 1 to recycling step 3, there was likely the most drastic reduction in fiber length whilst the reduction had likely plateaued relatively speaking by this point, with the increased crystallinity of the PLA further explaining the increase from step 3 to step 6.

3.4. Impact Strength of Injection-Molded Samples

The toughness of the samples was evaluated by assessing the impact strength using the Charpy pendulum. As a property, impact strength is directly related to both mechanical resistant properties (δ_b) and ductile properties (ε_b). It is representative of the amount of energy a material can absorb during deformation prior to failure occurring. The impact strengths of the NFRCs are summarized in Table 5 and shown graphically in Figure 7. The effect of reprocessing steps on the impact strength of virgin PLA has been reported by Agüero et al. (2019) and Budin et al. (2019) whom reported the impact strength of neat PLA to decrease significantly with additional reprocessing steps. After four reprocessing steps, the impact strength had reduced by >50%. This lends credence to the importance of incorporating reinforcing agents to reduce the detrimental effect of reprocessing on the impact strength of PLA-based materials.

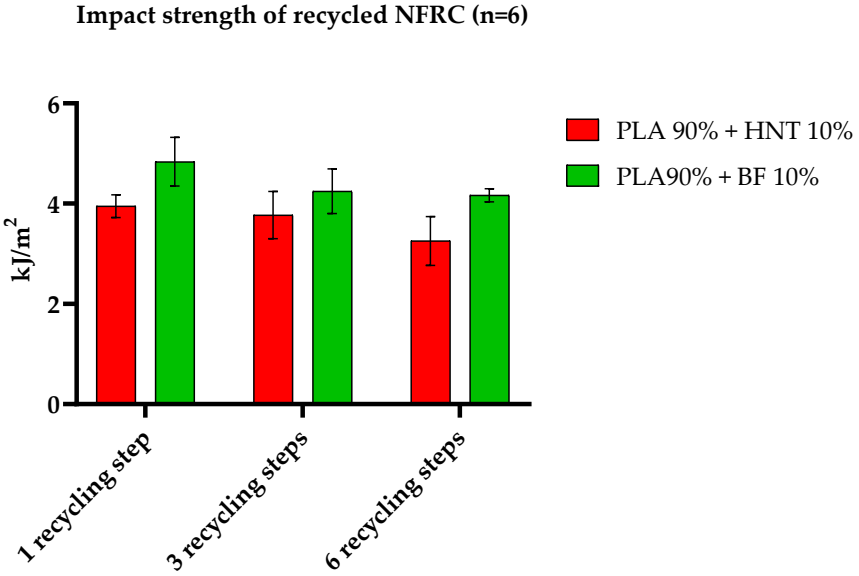

Figure 7. Comparison of the impact strength between PLA/HNT and PLA/BF composites recycled a total of 6 times (n = 6). (red) PLA 90 wt.% and HNT 10 wt.% and (green) PLA 90 wt.% and BF 10 wt.%.

The samples produced herein showed a decrease in impact strength with respect to increasing numbers of reprocessing steps. From 1 to 6 reprocessing cycles, the impact strength of PLA90/HNT10 reduced by 17.69%. Similarly, the impact strength of PLA90/BF10 reduced by 13.83%. The reduction in impact strength may be multifaceted in its cause. The additional reprocessing steps commonly lead to thermal degradation of PLA and a reduction in molecular weight [47,52]. However, it is common that reprocessing steps will lead to an increase in impact properties of NFRCs. A significant increase in impact strength of polypropylene-based NFRCs using coriander straw fibers, flax fibers, wood fibers and bagasse fibers has been shown in several studies [53–57]. This increase in impact strength has been attributed to the reduction in fiber length during the reprocessing steps, in turn leading to an increase in ductility of the samples. Like the results of this study, however, other researchers have observed the same trend whereby the impact strength of NFRCs has been negatively affected by the number of reprocessing steps. Post-reprocessing, both Graupner et al. (2016) and Fazita et al. (2015) have shown a reduction in impact strength of PLA-based composites when cellulose-fibers and bamboo-fibers were used, respectively. It has been posited by Evens et al. (2019) that the rationale for such a reduction may be related to the fiber length. They noted that certain fibers will increase the impact strength whilst others, such as glass fibers, will lead to a large reduction in impact strength. They go on to state that his may be due to the fiber's critical length, defined as the length required for the fiber to develop its fully stressed conditions in the polymer matrix. Should the fiber length be shorter than this critical length, it may slip from the polymer matrix [55].

3.5. Fracture Surface Morphology

The SEM images of HNT and BF-based NFRCs under 50 and 500× magnification are collected in Figure 8. Pristine PLA is known to be a brittle and stiff polymer with fractured surfaces displaying smooth laminated surfaces with little deformation upon fracture [29,58]. The SEM images of BF-based NFRCs display both pulled out fibers and voids left within the PLA matrix from the BF removal, suggesting poor adhesion between the fibers and matrix. In contrast, the HNT-based NFRCs display no holes, thus showing a much higher degree of adhesion. The three main mechanisms of energy absorption upon impact are (i) debonding, (ii) pull-out, and (iii) fiber fracture. The assumption is that strain energy released by fiber debonding and fracture has a proportional relationship with the debonded length. Therefore, a low level of adhesion between fiber and matrix results in a higher

degree of energy absorption [59]. The higher level of adhesion displayed by the HNT/PLA composites compared to that of the BF-based NFRCs would, therefore, be one explanation as to the greater impact strength displayed by the BF-loaded PLA composites [60].

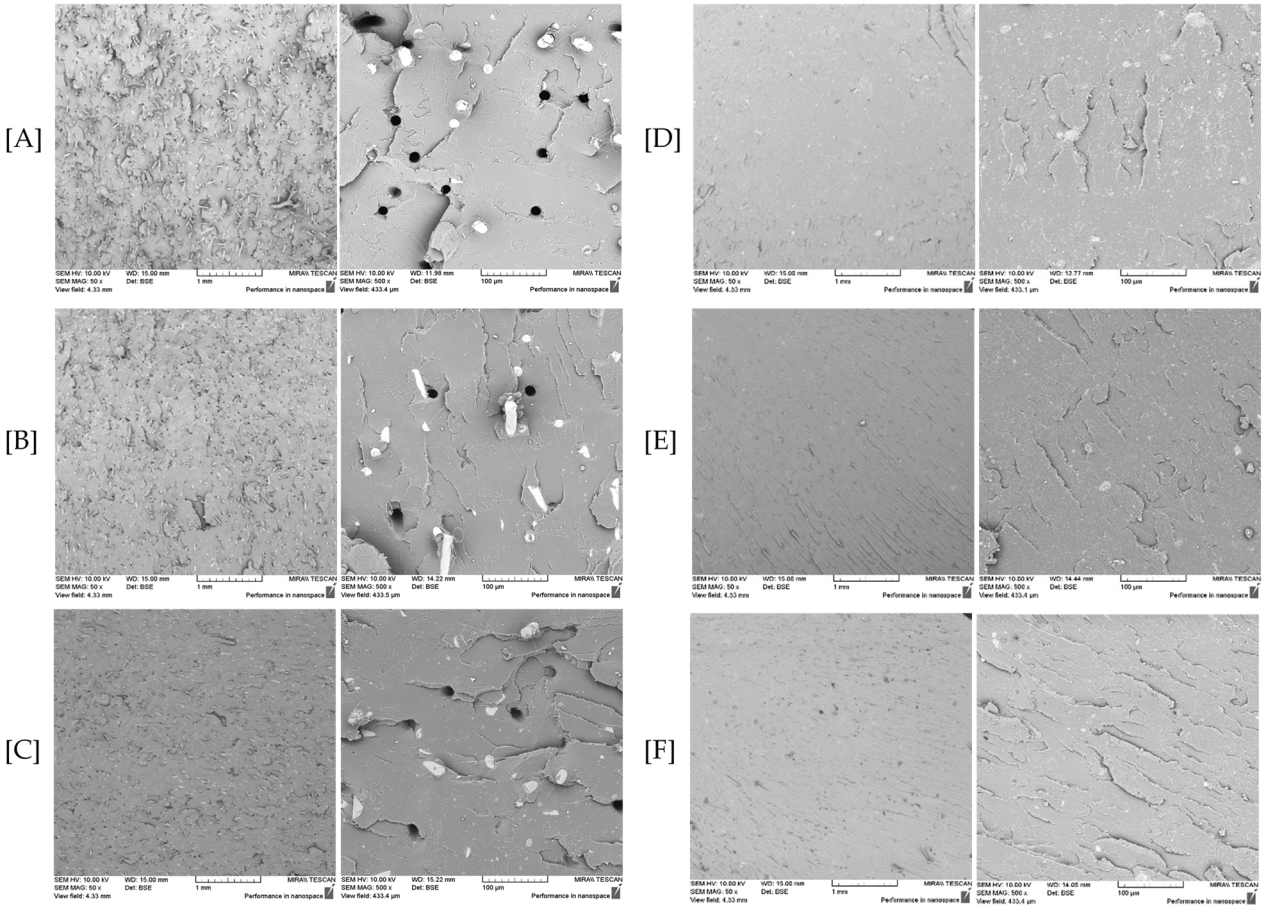

Figure 8. SEM images of the impact fracture of NFRCs. (L) 50× magnification, (R) 500× magnification; (**A**) 1 recycling step, (**B**) 3 recycling steps and (**C**) 6 recycling steps of BF-based NFRCs. (**D**) 1 recycling step, (**E**) 3 recycling steps and (**F**) 6 recycling steps of HNT-based NFRCs.

One of the major drawbacks regarding the use of natural fibers in polymer composites is the poor adhesion commonly observed between fiber and matrix, which subsequently results in poor tensile properties [61]. This is readily apparent in the BF-based samples. Though initially presenting greater tensile properties than those of the HNT-based samples, the tensile properties display a greater decrease upon further recycling steps. This "pull out" property of non-modified BFs has also been shown by other research teams [62]. The greater level of interfacial adhesion shown by HNTs meanwhile is the cause of the increase in tensile properties between recycling steps.

4. Conclusions

An initial investigation was conducted to study the feasibility of recycling polylactic acid (PLA)-based natural fiber-reinforced composites (NFRCs) through conical twin screw extrusion (CTSE). Despite the widespread use of PLA as a compostable polymer, it requires high temperatures (>50 °C) for degradation and is thus only compostable in industrial settings. Therefore, incorporating PLA waste into a recycling stream for re-use would increase its appeal. Two types of NFRCs based on basalt fibers and halloysite nanotubes were fabricated with a composite composition of 90 wt.% PLA and 10 wt.% reinforcing fiber, aiming to mitigate the most common defects that occur during polymeric material recycling, such as reduction in molecular weight or thermal degradation. The fabricated

composites underwent several mechanical recycling stages followed by injection molding to produce ASTM standard impact and tensile bars, which were subsequently analyzed for their properties. The study investigated the impact of mechanical recycling after one, three, and six recycling steps, with a consistent trend observed in the effect on mechanical properties. However, it is recommended to observe the second and fourth recycling steps to further expand upon the findings.

One of the initial observations in the mechanical recycling of virgin polylactic acid (PLA) is the deterioration and discoloration of the base polymer after subsequent reprocessing steps. This was further verified through color analysis, in which the ΔE^*_{ab} value for the tested specimens exceeded 5 with respect to the initial recyclate, indicating noticeable differences in color. Upon further literature review, it was discovered that this discoloration is the result of inevitable thermal degradation of PLA during the hot melt extrusion process, leading to the formation of carbonyl groups with conjugated double bonds. Depending on the end-application, this could have negative implications for the end-user, as a reduction in the appearance quality of the polymer may require the addition of colorants or even a change in end-application, both of which could impact the recyclability of PLA.

Both fiber-loaded composites demonstrated a reduction in impact strength with increasing recycling steps. This decline in performance was attributed to the decrease in fiber length resulting from the additional shear forces experienced during extrusion and molding processes, which is consistent with findings reported by Evens et al. (2019). The reduction in basalt fiber (BF) length was observed through SEM imaging, which revealed broken fibers and irregular voids left behind after fiber pull-out. Conversely, halloysite nanotubes (HNTs) displayed greater adhesion to PLA, which limited the extent of fiber pull-out during impact testing. However, the decrease in impact strength for HNT NFRCs could be attributed to both the reduction in fiber length and the negative impact of reprocessing on the PLA matrix. Virgin PLA is known to be a brittle polymer that exhibits a brittle fracture morphology with limited deformation. As evidenced by SEM imaging of the HNT/PLA composites, increasing recycling steps resulted in an increase in surface roughness and microfractures, indicative of an embrittlement process and decreased energy absorption during impact analysis.

The influence of reprocessing steps on the tensile properties of composite samples is a complex phenomenon that may result from multiple concomitant processes, such as poor fiber/matrix compatibility, reduction in fiber length, or thermal degradation of the PLA matrix. Poor interfacial adhesion between PLA and basalt fibers (BFs) was visually apparent under SEM, with the pulled-out BFs leaving behind distinct holes in the PLA matrix. It should be noted that the BFs used in this study were untreated, a known method for improving interfacial adhesion between PLA and BFs and greatly enhancing the tensile properties of composites. After further recycling and reduction of fiber lengths, a significant decrease in the tensile properties of BF-based samples was observed, whereas the samples using halloysite nanotubes (HNTs) did not exhibit this trend. SEM images of HNT composites showed a higher degree of adhesion between HNT and PLA matrix, leading to an increase in tensile properties up to three recycling steps. However, a slight decline in tensile properties was observed after six recycling steps, which was attributed to the onset of thermal degradation of the PLA and subsequent decline in material properties.

Overall, this research demonstrates that PLA and fiber-based composites can be recycled up to six times without significant detrimental effects on the mechanical properties of the final parts. Although this study presents a promising initial observation on the potential recyclability of BF- and HNT-based NFRCs, it has its limitations. As discussed throughout the paper, only a 10% (w/w) loading was used as the sole fiber loading. The fiber loading percentage could be increased in future research to enhance the mechanical properties of the formulations. Similarly, six recycling steps were used as the upper limit of mechanical recycling cycles in this study, but the true upper limit has not been conclusively identified. The tensile properties of BF composites showed a drastic decline after three recycling steps, but no surface modification was made to the BFs prior to material

processing, which is a known method for improving interfacial adhesion between PLA and BFs. To improve the recyclability of BF/PLA composites, chemical surface treatment may be initially implemented.

Author Contributions: Conceptualization, J.F.; Formal analysis, J.F.; Investigation, J.F., V.C., A.P., S.R., T.H., S.C., G.S.N.B. and C.D.; Methodology, J.F.; Supervision, P.M. and D.M.C.; Writing—original draft, J.F. and G.S.N.B.; Writing—review and editing, D.M.D., N.M.G. and D.M.C. All authors have read and agreed to the published version of the manuscript.

Funding: This research received no external funding.

Data Availability Statement: Not applicable.

Conflicts of Interest: The authors declare no conflict of interest.

References

1. Hundertmark, T.; Mayer, M.; McNally, C.; Simons, T.J.; Witte, C. How Plastics Waste Recycling Could Transform the Chemical Industry, 12 December 2018. Available online: https://www.mckinsey.com/industries/chemicals/our-insights/how-plastics-waste-recycling-could-transform-the-chemical-industry (accessed on 25 January 2023).
2. Zhang, Y.; Pu, S.; Lv, X.; Gao, Y.; Ge, L. Global trends and prospects in microplastics research: A bibliometric analysis. *J. Hazard. Mater.* **2020**, *400*, 123110. [CrossRef] [PubMed]
3. Shen, M.; Huang, W.; Chen, M.; Song, B.; Zeng, G.; Zhang, Y. (Micro)plastic crisis: Un-ignorable contribution to global greenhouse gas emissions and climate change. *J. Clean. Prod.* **2020**, *254*, 120138. [CrossRef]
4. Almroth, B.; Eggert, H. Marine Plastic Pollution: Sources, Impacts, and Policy Issues. *Rev. Environ. Econ. Policy* **2019**, *13*, 317–326. [CrossRef]
5. Brooks, A.L.; Wang, S.; Jambeck, J.R. The Chinese import ban and its impact on global plastic waste trade. *Sci. Adv.* **2018**, *4*, eaat0131. [CrossRef]
6. Vroman, I.; Tighzert, L. Biodegradable Polymers. *Materials* **2009**, *2*, 307–344. [CrossRef]
7. Ubeda, S.; Aznar, M.; Nerín, C. Determination of volatile compounds and their sensory impact in a biopolymer based on polylactic acid (PLA) and polyester. *Food Chem.* **2019**, *294*, 171–178. [CrossRef]
8. Panseri, S.; Martino, P.A.; Cagnardi, P.; Celano, G.; Tedesco, D.; Castrica, M.; Balzaretti, C.; Chiesa, L.M. Feasibility of biodegradable based packaging used for red meat storage during shelf-life: A pilot study. *Food Chem.* **2018**, *249*, 22–29. [CrossRef]
9. Averous, L. Polylactic Acid: Synthesis, Properties and Applications. In *Monomers, Polymers and Composites from Renewable Resources*; Elsevier: Aveiro, Portugal, 2008; pp. 433–450.
10. Taib, N.-A.A.B.; Rahman, R.; Huda, D.; Kuok, K.K.; Hamdan, S.; Bin Bakri, M.K.; Bin Julaihi, M.R.M.; Khan, A. A review on poly lactic acid (PLA) as a biodegradable polymer. *Polym. Bull.* **2022**, *80*, 1179–1213. [CrossRef]
11. Cristea, M.; Ionita, D.; Iftime, M.M. Dynamic Mechanical Analysis Investigations of PLA-Based Renewable Materials: How Are They Useful? *Materials* **2020**, *13*, 5302. [CrossRef]
12. Aldhafeeri, T.; Alotaibi, M.; Barry, C.F. Impact of Melt Processing Conditions on the Degradation of Polylactic Acid. *Polymers* **2022**, *14*, 2790. [CrossRef]
13. Yu, W.; Wang, X.; Ferraris, E.; Zhang, J. Melt crystallization of PLA/Talc in fused filament fabrication. *Mater. Des.* **2019**, *182*, 108013. [CrossRef]
14. Bakar, A.A.B.A.; Zainuddin, M.Z.B.; AAdam, N.B.; Noor, I.S.B.M.; Tamchek, N.B.; Alauddin, M.S.B.; Ghazali, M.I.B.M. The study of mechanical properties of poly(lactic) acid PLA-based 3D printed filament under temperature and environmental conditions. *Mater. Today Proc.* **2022**, *67*, 652–658. [CrossRef]
15. Pilla, S.; Gong, S.; O'Neill, E.; Yang, L.; Rowell, R.M. Polylactide-recycled wood fiber composites. *J. Appl. Polym. Sci.* **2008**, *111*, 37–47. [CrossRef]
16. Bajpai, P.K.; Singh, I.; Madaan, J. Comparative studies of mechanical and morphological properties of polylactic acid and polypropylene based natural fiber composites. *J. Reinf. Plast. Compos.* **2012**, *31*, 1712–1724. [CrossRef]
17. Hu, R.; Lim, J.-K. Fabrication and Mechanical Properties of Completely Biodegradable Hemp Fiber Reinforced Polylactic Acid Composites. *J. Compos. Mater.* **2007**, *41*, 1655–1669. [CrossRef]
18. Huda, M.S.; Drzal, L.T.; Mohanty, A.K.; Misra, M. Effect of fiber surface-treatments on the properties of laminated biocomposites from poly(lactic acid) (PLA) and kenaf fibers. *Compos. Sci. Technol.* **2008**, *68*, 424–432. [CrossRef]
19. Singh, J.I.P.; Singh, S.; Dhawan, V. Influence of fiber volume fraction and curing temperature on mechanical properties of jute/PLA green composites. *Polym. Polym. Compos.* **2020**, *28*, 273–284. [CrossRef]
20. Khandelwal, S.; Rhee, K.Y. Recent advances in basalt-fiber-reinforced composites: Tailoring the fiber-matrix interface. *Compos. Part B Eng.* **2020**, *192*, 108011. [CrossRef]
21. Saleem, A.; Medina, L.; Skrifvars, M.; Berglin, L. Hybrid Polymer Composites of Bio-Based Bast Fibers with Glass, Carbon and Basalt Fibers for Automotive Applications—A Review. *Molecules* **2020**, *25*, 4933. [CrossRef]

22. Najjar, I.; Sadoun, A.; Elaziz, M.A.; Abdallah, A.; Fathy, A.; Elsheikh, A.H. Predicting kerf quality characteristics in laser cutting of basalt fibers reinforced polymer composites using neural network and chimp optimization. *Alex. Eng. J.* **2022**, *61*, 11005–11018. [CrossRef]
23. Fakhruddin, K.; Hassan, R.; Khan, M.U.A.; Allisha, S.N.; Razak, S.I.A.; Zreaqat, M.H.; Latip, H.F.M.; Jamaludin, M.N.; Hassan, A. Halloysite nanotubes and halloysite-based composites for biomedical applications. *Arab. J. Chem.* **2021**, *14*, 103294. [CrossRef]
24. Ye, Y.; Chen, H.; Wu, J.; Ye, L. High impact strength epoxy nanocomposites with natural nanotubes. *Polymer* **2007**, *48*, 6426–6433. [CrossRef]
25. Chee, S.S.; Jawaid, M.; Sultan, M.; Alothman, O.Y.; Abdullah, L.C. Effects of nanoclay on physical and dimensional stability of Bamboo/Kenaf/nanoclay reinforced epoxy hybrid nanocomposites. *J. Mater. Res. Technol.* **2020**, *9*, 5871–5880. [CrossRef]
26. Joussein, E.; Petit, S.; Churchman, J.; Theng, B.; Righi, D.; Delvaux, B. Halloysite clay minerals: A review. *Clay Miner.* **2005**, *40*, 383–426. [CrossRef]
27. Chao, C.; Liu, J.; Wang, J.; Zhang, Y.; Zhang, B.; Zhang, Y.; Xiang, X.; Chen, R. Surface Modification of Halloysite Nanotubes with Dopamine for Enzyme Immobilization. *ACS Appl. Mater. Interfaces* **2013**, *5*, 10559–10564. [CrossRef] [PubMed]
28. Hopmann, C.; Schippers, S.; Hofs, C. Influence of Recycling of Poly(lactic acid) on Packaging. *J. Appl. Polym. Sci.* **2014**, *132*. [CrossRef]
29. Agüero, A.; Morcillo, M.d.C.; Quiles-Carrillo, L.; Balart, R.; Boronat, T.; Lascano, D.; Torres-Giner, S.; Fenollar, O. Study of the Influence of the Reprocessing Cycles on the Final Properties of Polylactide Pieces Obtained by Injection Molding. *Polymers* **2019**, *11*, 1908. [CrossRef] [PubMed]
30. Mysiukiewicz, O.; Barczewski, M.; Skórczewska, K.; Matykiewicz, D. Correlation between Processing Parameters and Degradation of Different Polylactide Grades during Twin-Screw Extrusion. *Polymers* **2020**, *12*, 1333. [CrossRef]
31. Gonçalves, L.M.G.; Rigolin, T.R.; Frenhe, B.M.; Bettini, S.H.P. On the Recycling of a Biodegradable Polymer: Multiple Extrusion of Poly (Lactic Acid). *Mater. Res.* **2020**, *23*. [CrossRef]
32. Peike, C.; Kaltenbach, T.; Weiß, K.; Koehl, M. Indoor vs. Outdoor Aging: Polymer Degradation in pv Modules Investigated by Raman Spectroscopy. *Proc. SPIE* **2012**, *8472*, 84720V.
33. Yousif, E.; Haddad, R. Photodegradation and photostabilization of polymers, especially polystyrene. *SpringerPlus* **2013**, *2*, 398. [CrossRef] [PubMed]
34. Stencel, R.; Kasperski, J.; Pakieła, W.; Mertas, A.; Bobela, E.; Barszczewska-Rybarek, I.; Chladek, G. Properties of Experimental Dental Composites Containing Antibacterial Silver-Releasing Filler. *Materials* **2018**, *11*, 1031. [CrossRef] [PubMed]
35. Mokrzycki, W.; Tatol, M. Color difference Delta E—A survey. *Mach. Graph. Vis.* **2011**, *20*, 383–411.
36. Carrasco, F.; Pagès, P.; Gámez-Pérez, J.; Santana, O.; Maspoch, M. Processing of poly(lactic acid): Characterization of chemical structure, thermal stability and mechanical properties. *Polym. Degrad. Stab.* **2010**, *95*, 116–125. [CrossRef]
37. Borovikov, P.; Sviridov, A.; Antonov, E.; Dunaev, A.; Krotova, L.; Fatkhudinov, T.; Popov, V. Model of aliphatic polyesters hydrolysis comprising water and oligomers diffusion. *Polym. Degrad. Stab.* **2019**, *159*, 70–78. [CrossRef]
38. Silva, A.L.N.; Cipriano, T.F.; Silva, A.H.M.F.T.d.; Sousa, A.M.F.; Silva, G.M. Thermal, rheological and morphological properties of poly (lactic acid) (PLA) and talc composites. *Polímeros* **2014**, *24*, 276–282. [CrossRef]
39. Zhang, G.G.Z. Phase transformation considerations during process development and manufacture of solid oral dosage forms. *Adv. Drug Deliv. Rev.* **2004**, *56*, 371–390. [CrossRef]
40. Bezerra, G.; de Lima, T.D.M.; Colbert, D.; Geever, J.; Geever, L. Formulation and Evaluation of Fenbendazole Extended-Release Extrudes Processed by Hot-Melt Extrusion. *Polymers* **2022**, *14*, 4188. [CrossRef]
41. Lim, L.-T.; Auras, R.; Rubino, M. Processing technologies for poly(lactic acid). *Prog. Polym. Sci.* **2008**, *33*, 820–852. [CrossRef]
42. Bakkal, M.; Bodur, M.S.; Berkalp, O.B.; Yilmaz, S. The effect of reprocessing on the mechanical properties of the waste fabric reinforced composites. *J. Mater. Process. Technol.* **2012**, *212*, 2541–2548. [CrossRef]
43. Huang, P.-W.; Peng, H.-S. Number of Times Recycled and Its Effect on the Recyclability, Fluidity and Tensile Properties of Polypropylene Injection Molded Parts. *Sustainability* **2021**, *13*, 11085. [CrossRef]
44. Balani, K.; Verma, V.; Agarwal, A.; Narayan, R. Physical, Thermal, and Mechanical Properties of Polymers. In *Biosurfaces: A Materials Science and Engineering Perspective*; Balani, K., Verma, V., Agarwal, A., Narayan, R., Eds.; John Wiley & Sons, Inc: Hoboken, NJ, USA, 2015; pp. 329–344.
45. Chen, Y.; Geever, L.M.; Killion, J.A.; Lyons, J.G.; Higginbotham, C.L.; Devine, D.M. Halloysite nanotube reinforced polylactic acid composite. *Polym. Compos.* **2015**, *38*, 2166–2173. [CrossRef]
46. Miwa, M.; Horiba, N. Effects of fibre length on tensile strength of carbon/glass fibre hybrid composites. *J. Mater. Sci.* **1994**, *29*, 973–977. [CrossRef]
47. Graupner, N.; Albrecht, K.; Ziegmann, G.; Enzler, H.; Muessig, J. Influence of reprocessing on fibre length distribution, tensile strength and impact strength of injection moulded cellulose fibre-reinforced polylactide (PLA) composites. *Express Polym. Lett.* **2016**, *10*, 647–663. [CrossRef]
48. Åkesson, D.; Vrignaud, T.; Tissot, C.; Skrifvars, M. Mechanical Recycling of PLA Filled with a High Level of Cellulose Fibres. *J. Polym. Environ.* **2016**, *24*, 185–195. [CrossRef]
49. Bajwa, D.; Bhattacharjee, S. Impact of recycling on the mechanical and mechanical properties of wood fiber based HDPE and PLA composites. In *Handbook of Composites from Renewable Materials*; Scivener Publishing LLC: Beverly, MA, USA, 2017; pp. 271–292.

50. Baek, B.S.; Park, J.W.; Lee, B.H.; Kim, H.J. Development and Application of Green Composites: Using Coffee Ground and Bamboo Flour. *J. Polym. Environ.* **2013**, *21*, 702–709. [CrossRef]
51. Kumar, A.; Tumu, V.R. Physicochemical Properties of the Electron Beam Irradiated Bamboo Powder and Its Bio-Composites with PLA. *Compos. Part B Eng.* **2019**, *175*, 107098. [CrossRef]
52. Awale, R.J.; Ali, F.B.; Azmi, A.S.; Puad, N.I.M.; Anuar, H.; Hassan, A. Enhanced Flexibility of Biodegradable Polylactic Acid/Starch Blends Using Epoxidized Palm Oil as Plasticizer. *Polymers* **2018**, *10*, 977. [CrossRef]
53. Uitterhaegen, E.; Parinet, J.; Labonne, L.; Mérian, T.; Ballas, S.; Véronèse, T.; Merah, O.; Talou, T.; Stevens, C.V.; Chabert, F.; et al. Performance, durability and recycling of thermoplastic biocomposites reinforced with coriander straw. *Compos. Part A Appl. Sci. Manuf.* **2018**, *113*, 254–263. [CrossRef]
54. Gourier, C.; Bourmaud, A.; Le Duigou, A.; Baley, C. Influence of PA11 and PP thermoplastic polymers on recycling stability of unidirectional flax fibre reinforced biocomposites. *Polym. Degrad. Stab.* **2017**, *136*, 1–9. [CrossRef]
55. Evens, T.; Bex, G.-J.; Yigit, M.; De Keyzer, J.; Desplentere, F.; Van Bael, A. The Influence of Mechanical Recycling on Properties in Injection Molding of Fiber-Reinforced Polypropylene. *Int. Polym. Process.* **2019**, *34*, 398–407. [CrossRef]
56. Soccalingame, L.; Perrin, D.; Bénézet, J.; Mani, S.; Coiffier, F.; Richaud, E.; Bergeret, A. Reprocessing of artificial UV-weathered wood flour reinforced polypropylene composites. *Polym. Degrad. Stabil.* **2015**, *120*, 313–327. [CrossRef]
57. Correa-Aguirre, J.; Luna-Vera, F.; Caicedo, C.; Vera-Mondragón, B.; Hidalgo-Salazar, M. The Effects of Reprocessing and Fiber Treatments on the Properties of Polypropylene-Sugarcane Bagasse Biocomposites. *Polymers* **2020**, *12*, 1440. [CrossRef] [PubMed]
58. Gao, H.; Qiang, T. Fracture Surface Morphology and Impact Strength of Cellulose/PLA Composites. *Materials* **2017**, *10*, 624. [CrossRef]
59. Thomason, J.; Vlug, M. Influence of fibre length and concentration on the properties of glass fibre-reinforced polypropylene: 4. Impact properties. *Compos. Part A: Appl. Sci. Manuf.* **1997**, *28*, 277–288. [CrossRef]
60. Bax, B.; Müssig, J. Impact and tensile properties of PLA/Cordenka and PLA/flax composites. *Compos. Sci. Technol.* **2008**, *68*, 1601–1607. [CrossRef]
61. Ku, H.; Wang, H.; Pattarachaiyakoop, N.; Trada, M. A review on the tensile properties of natural fiber reinforced polymer composites. *Compos. Part B Eng.* **2011**, *42*, 856–873. [CrossRef]
62. Kuciel, S.; Mazur, K.; Hebda, M. The Infuence of Wood and Basalt Fibres on Mechanical, Thermal and Hydrothermal Properties of PLA Composites. *J. Polym. Environ.* **2020**, *28*, 1204–1215. [CrossRef]